Evolution of Kink Bands and Tilt Boundaries in Block Copolymers at Large Shear Strains

Lei Qiao and Karen I. Winey*

Laboratory for Research on the Structure of Matter, Department of Materials Science and Engineering, University of Pennsylvania, Philadelphia, Pennsylvania 19104-6272

Received August 4, 1999; Revised Manuscript Received December 6, 1999

ABSTRACT: The evolution of kink bands and kink band boundaries in a prealigned poly(styrene-*b*-ethylene propylene) lamellar diblock copolymer was investigated by applying steady shear at strains in the range of 1−10 strain units. Boundary morphologies were characterized using transmission electron microscopy. As the shear strain increases, both the kink bands and the lamellae within the kink bands rotate continuously toward the shearing direction, leading to a decrease in the tilt boundary angle and the kink band boundary angle. Simultaneously, the nature of the kink band boundary transforms. The chevron boundaries present at low strains, and thus large tilt angles, become omega boundaries as the strain increases to ∼3 strain units. At higher strains (∼5 strain units), the tilt angle further decreases, and the omega boundaries start to break, preferentially in the PS microdomains. Delamination of the PS microdomains was also observed at the highest strain amplitude (10 strain units), which was associated with the limited extent of entanglement across the PS microdomains.

Introduction

The equilibrium morphologies in diblock copolymers are known to depend on the volume fraction, the total molecular weight, and the interaction parameter of the material. These microphase-separated morphologies are well-documented for a variety of materials in the weak, intermediate, and strong segregation limits. Presently, block copolymers are being considered for a variety of applications that would use their nanostructured morphologies. The optical, permeability, and electrical properties of microphase-separated block copolymers depend on the chemical species, the morphology type (lamellae, gyroid, cylinders, etc.), the global orientation of the morphology, and the topological defects in the morphology. Of these four controlling factors, topological defects in block copolymers have received the least attention. The importance of defects is twofold. The type, size, and density of defects in block copolymers alter the macroscopic properties. Furthermore, many of these materials are likely to be processed in their microphase-separated state in which the motion and transformation of defects determines the plasticity of the diblock copolymers.

Experimental and theoretical efforts to understand defects, particularly grain boundaries, have been made for the quiescent state of block copolymers.[1−3] Specifically, Gido and Thomas studied the tilt boundary, which is the most common boundary type in lamellar diblock copolymers. They reported three types of tilt boundary morphologies in a poly(styrene-*b*-butadiene) diblock copolymer: the chevron tilt boundary, in which lamellae bend smoothly across the grain boundary; the omega tilt boundary, in which one of the microdomains forms protrusions while the other microdomain forms Ω-shaped caps around the protrusions; and finally, the T-junction in which the lamellae are discontinuous across the boundary as the tilt boundary becomes highly asymmetric.[1] They also observed that the chevron tilt boundaries exist predominately at high tilt angles while the omega boundaries exist at lower boundary angles. Matsen subsequently examined the first two types of tilt boundaries theoretically using a self-consistent-field theory.[2] He also found an evolution in the microdomain shape from the chevron to the omega boundary as the tilt angle decreases. Matsen explained this morphological transition in terms of three energy contributions: the interfacial bending energy between A/B microdomains, the interfacial tension, and packing frustration.

Unlike the study of a single grain boundary in a block copolymer sample annealed quiescently, Polis and Winey have studied kink bands in a lamellar block copolymer in the presence of an external shear field.[4,5] These shear-induced kink bands consist of pairs of opposite tilt boundaries separated by a width of ∼0.5 μm. Kink bands are an important low-energy defect structure in lamellar diblock copolymers[2,6] and the origin of the previously observed parallel−transverse biaxial texture.[4,7−9] These defects initiate in prealigned block copolymers when the shear strain exceeds a critical value[5] and grow through a lamellar rotation mechanism.[10] These previous studies focused on the initiation of kink bands and the early stages of kink band growth with strains less than 1 strain unit. In contrast, we report the evolution of kink bands in a lamellar diblock copolymer under steady shear in the range of 1−10 strain units; specifically we examine the morphological transformations at the kink band boundaries.

Experimental Section

Sample Preparation. The polymer used in this study was poly(styrene-*b*-ethylene propylene) diblock copolymer (Kraton G1701), provided by Shell Chemical Co. It was previously used by Polis and Winey[4,5] to study kink bands at <100% shear strain. It has a weight-averaged molecular weight of 110 000 g/mol with 37 wt % styrene monomeric unit content. The copolymer will be referred to as SEP(40−70), corresponding to the nominal molecular weights of the PS and PEP blocks. Films ∼1 mm thick of SEP(40−70) having less than 1 wt % Irganox 1010 were cast at room temperature from a 5 wt % toluene solution. (Irganox 1010 is an antioxidant supplied by

* Corresponding author. E-mail winey@lrsm.upenn.edu.

10.1021/ma991303k CCC: $19.00
Published on Web 01/22/2000

Ciba Geigy.) The films were dried under vacuum for 24 h at room temperature, followed by 24 h at 120 °C, and annealed at 150 °C for 48 h. The samples were compression molded before the reciprocating shear and steady shear experiments. The morphology after annealing and molding is lamellar with a long period of ~70 nm, as determined from small-angle X-ray scattering.

Rheology. A shearing device was designed to apply reciprocating shear for the alignment of block copolymers and steady shear for the systematic creation of defects in these block copolymers. This parallel plate device has an adjustable gap, linear (as opposed to rotational) motion, a range of shearing frequencies, and a large strain capability (up to 20 strain units). Our large-strain shearing device mimics the geometry of the Rheometrics RSA II used in our previous studies in which the shear stain is uniform across the specimen. Following a previous protocol established by Polis et al.,[5] a strain-ramping large-amplitude reciprocating shear was used to create a nearly parallel starting state: strain amplitudes of 20% for 15 min and then 40% for 45 min were applied at 180 °C and a frequency of 1 rad/s. After the reciprocating shear procedure, samples were annealed for ~1.5 h before conducting steady-shear experiments. Steady shear was applied at a fixed rate of 0.001 s^{-1} for a series of strain amplitudes, ranging from 1 to 10 strain units. Immediately after the steady shear, samples were quenched to room temperature by liquid nitrogen for further morphological examination.

Transmission Electron Microscopy. Transmission electron microscopy was used to examine kink band boundary morphologies at large strains. A block of ~5 × 5 mm was cut and mounted on a specimen stub with the 3-direction (or neutral direction) normal to the stub surface, because this orientation provides cross sections of kink bands. A small mesa of ~0.5 × 0.5 mm was then created on the block face using a Reichert Ultracut cryo-ultramicrotome operated at −100 °C. Thin sections of ~60 nm were microtomed and collected, followed by staining in a RuO_4 vapor, which preferentially stains the PS microdomains to enhance mass contrast. A Philips 400T transmission electron microscope, operated at 100 kV, was used for detailed observation of kink boundary morphologies. Negatives from the electron microscopy were scanned to create digital image files; therefore, the PS microdomains appear bright in the images.

Results

Three orthogonal orientations have been defined relative to the shearing direction for lamellar block copolymers. When the normal to the lamellae is along the shear gradient direction, which is labeled the 2-direction, the orientation is called parallel. Alternatively, when the normals of the lamellae are along the shear direction (1-direction) or the neutral direction (3-direction), the orientations are called transverse and perpendicular, respectively. The protocol of strain-ramping large-amplitude reciprocating shear produced a predominately parallel orientation in this strongly microphase-separated diblock copolymer, SEP(40−70) (Figure 1). Despite some remaining defects and misaligned lamellae, the predominately parallel orientation is obvious in the micrograph and simplifies the detection and analysis of kink bands as the sample is subjected to steady shear. Note that all the micrographs presented in this paper are of the 1−2 plane (shear−shear gradient plane), which best depicts the kink band morphology in the lamellae.

Figure 2 displays an individual forward kink band in SEP(40−70) following 100% shear strain at a shear rate of 0.001 s^{-1} and 180 °C. We characterize the kink bands by the tilt boundary angle or tilt angle, θ, which is the angle between lamellae inside a kink band and lamellae adjacent to the kink band, as shown in Figure 2. A total of six angles were measured along the upper and lower boundaries of a kink band, and the average was taken as the tilt angle for this particular kink band. After 100% strain, the tilt angles are between 60° and 110°. Polis et al. reported tilt angles in the range of 100°−160° in the same block copolymer subjected to somewhat less shear strain (40%−80%).[5] An apparent decrease in the tilt angle occurs as shear strain increases from 40% to 100%. In contrast, the average width of the kink bands, i.e., the distance between the upper and lower boundaries of the kink bands, is ~0.5 μm independent of the applied strain up to 100%. All the kink band boundaries created by ≤100% strain exhibit the chevron boundary type.

The evolution of kink bands was followed to larger shear strains from 1 to 10 strain units. After a shear deformation of 3 strain units, the kink band boundaries exhibit a further decrease in the tilt angle (30°−110°)

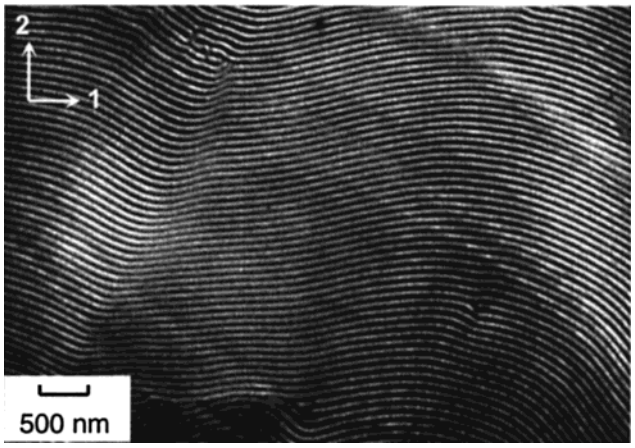

Figure 1. TEM image of the 1−2 plane (i.e., shear−shear gradient plane) in SEP(40−70) following the strain-ramping alignment procedure. Lamellae normals are along the 2-direction, corresponding to a predominately parallel starting state. In this and subsequent micrographs, the PS microdomains appear brighter, because PS was selectively stained by RuO_4 and this is a negative.

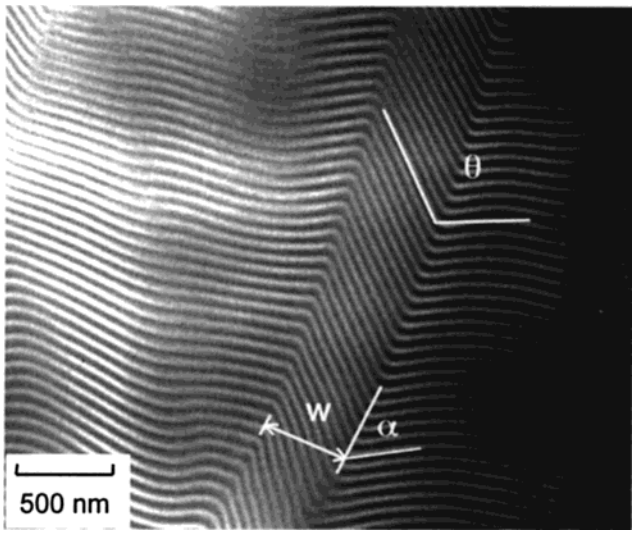

Figure 2. TEM image of an individual forward kink band in a prealigned SEP(40−70) sample subjected to steady shear at 180 °C, 0.001 s^{-1}, and 1 strain unit. The 1−2 plane is shown. The average tilt boundary angle of this kink band, i.e., the angle between the lamellae inside and adjacent to the kink band, θ, is ~107°.

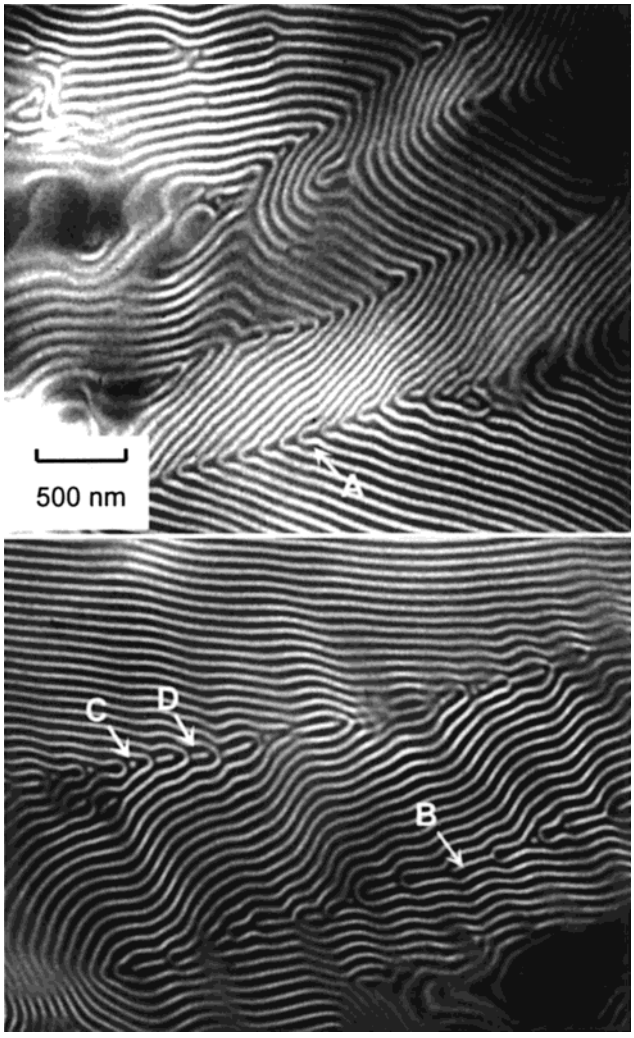

Figure 3. TEM image of a kink band in a prealigned SEP-(40−70) sample subjected to steady shear at 180 °C, 0.001 s^{-1}, and 3 strain units. The 1−2 plane is shown. Four types of omega morphologies are observed. Standard omega boundary morphology, in which the protrusions in the PEP microdomains (black) are covered by the omega-shaped PS caps (white) (A). Omega boundary with extra PS microdomains, either connected (B) or disconnected in the shape of cylinders (C) or short lamellae (D). Periodic undulations of lamellae were found emanating from the kink band.

and a transition in the tilt boundary morphology (Figure 3). The boundary transforms from a chevron to an omega-type tilt boundary as the strain increases and the tilt angle decreases. Four types of omega boundary morphologies are prevalent in the sample subjected to 3 strain units, as indicated by regions A−D in Figure 3. Region A shows the standard omega boundary morphology, in which protrusions in the PEP layers (black) are covered by arching PS layers (white). The omega-shaped caps are preferentially in the PS microdomains. Other regions display boundaries in which the PS omega shape exhibits a protrusion that is connected or disconnected. Region B is an example having the protrusion connected to the PS omega; this protrusion causes the PEP layer to be distorted into a pseudo-omega shape. Alternatively, the PS protrusion can be disconnected so that it could also be described as an extra or interstitial PS microdomain. These interstitial PS microdomains can be either cylinders (C) or short lamellae (D). These four types of omega boundaries are found in roughly equal amounts in the SEP(40−70) sheared to 3 strain units. Furthermore, periodic undulations exist in the lamellae adjacent to the kink band at this strain amplitude (Figure 3) as well as at higher strains (Figures 4 and 5). These undulations could be due to lamellar relaxations in response to shear-induced layer contraction.[11]

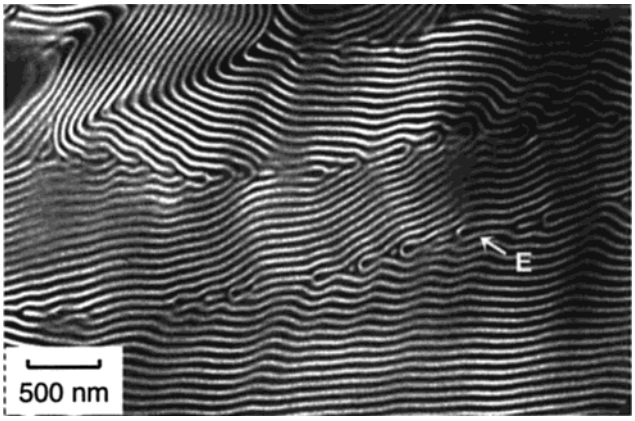

Figure 4. TEM image of a kink band in a prealigned SEP-(40−70) sample subjected to steady shear at 180 °C, 0.001 s^{-1}, and 5 strain units. The 1−2 plane is shown. Both the protrusions in the PEP microdomains and the omega caps in the PS microdomains of the tilt boundaries are elongated (E) as compared to those at 3 strain units.

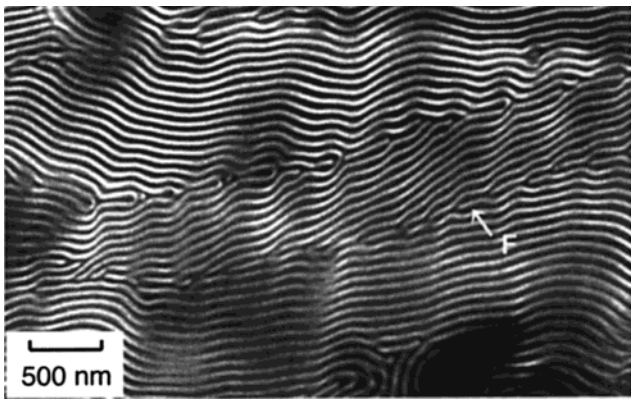

Figure 5. TEM image of a kink band in a prealigned SEP-(40−70) sample subjected to steady shear at 180 °C, 0.001 s^{-1}, and 10 strain units, showing broken omega boundaries in the PS microdomains (F). The 1−2 plane is shown.

Kink bands persist at larger strains as shown in Figures 4 and 5. The tilt boundary angles continue to decrease from an average of ∼55° to ∼25° as the strain increases from 5 to 10 strain units. The omega-type boundaries are still prevalent at these strain amplitudes. Both the protrusions and the omega caps at the boundary are more extended or elongated as compared to those produced at 3 strain units; for example, compare A in Figure 3 and E in Figure 4. In addition, lamellae break along the center of some omega boundaries, and the occurrence of these broken lamellae is always in the PS microdomains; see region F in Figure 5. This breaking phenomenon in polystyrene microdomains indicates that polystyrene is the weaker microdomain during steady shear at 180 °C, as will be discussed further. Moreover, at strain amplitudes above 3 strain units, and especially in the sample with 10 strain units, we observed a delamination behavior along the center of some microdomains, as shown in Figure 6. This delamination was found exclusively in the PS microdomains.

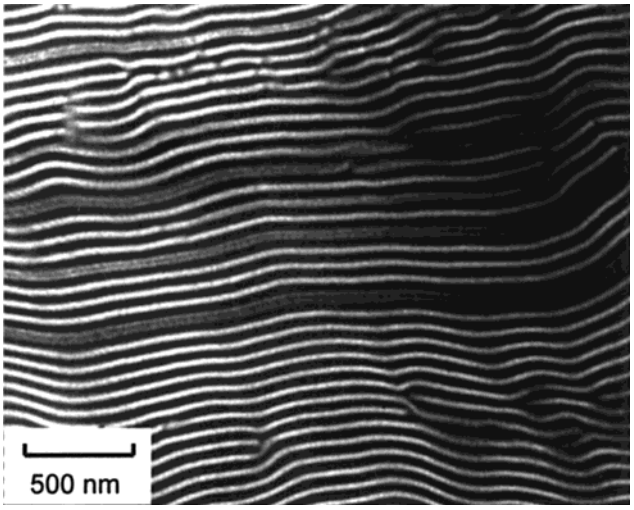

Figure 6. TEM image of a kink band in a prealigned SEP-(40−70) sample subjected to steady shear at 180 °C, 0.001 s^{-1}, and 10 strain units, showing delamination in the PS microdomains. The 1−2 plane is shown.

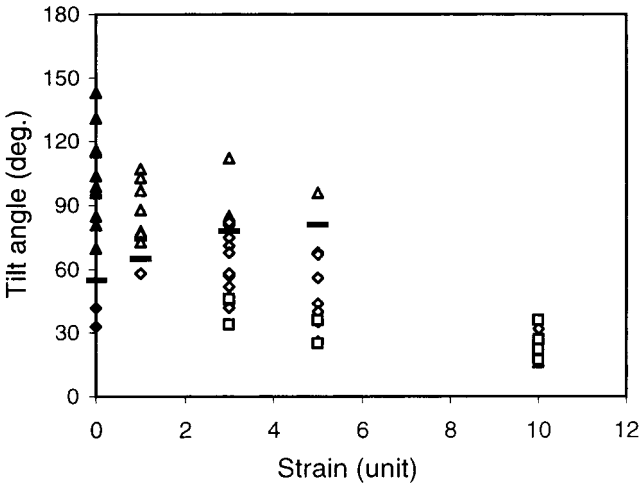

Figure 7. Tilt boundary angle (θ) versus strain amplitude measured from TEM images of SEP(40−70) in both as-cast and annealed samples (filled symbols) and samples subjected to large steady shear strains (open symbols). The tilt boundary angle decreases as strain amplitude increases, accompanied by a transition in the tilt boundary morphology, from chevron (triangle) to omega (diamond), and finally to broken lamellae (square). The transitions between the chevron and omega boundary morphologies are indicated by horizontal bars and are found to increase with applied shear strain.

Figure 7 shows the tilt boundary angles as a function of applied shear strain and also indicates the type of tilt boundary morphology. The tilt angles measured at zero strain represent measurements from a solvent cast and annealed SEP(40−70) sample, so that the tilt boundaries are grain boundaries rather than kink band boundaries. As expected, our values at zero strain compare favorably with Gido's quiescent study.[1] Most of the grain boundaries observed in the quiescent case are chevron tilt boundaries, as expected because of the higher energy associated with the omega boundary morphology.[2] Although a range of angles is observed for each strain, an overall decrease in the tilt boundary angles is evident as the strain amplitude increases, from an average of ∼85° at 1 strain unit to ∼25° at 10 strain units. Furthermore, the decrease in the tilt boundary angle is accompanied by transitions in the tilt boundary morphologies, from chevron to omega morphologies, and finally to a broken omega morphology. While these transitions appear to exist over a range of angles, the critical tilt angle between the chevron and omega boundaries increases somewhat with applied strain, as indicated by the horizontal bars in Figure 7.

Discussion

Effect of Strain on Kink Band Morphology and Alignment. The kink band morphology and kink bandwidth (∼0.5 μm) persist at large strains, while the average tilt boundary angle decreases from an average of ∼85° at 1 strain unit to ∼25° at 10 strain units. This reduction in the tilt boundary angle is in agreement with previous work, in which the lamellae within kink bands were found to rotate during shear strains up to 80%.[10] In addition, the kink band boundary angle α, which is the angle between the kink band boundary and lamellae adjacent to the kink band, decreases during steady shear (Figure 2). For example, α is ∼45° at 1 strain unit and ∼10° at 10 strain units. This indicates that not only are the lamellae inside the kink bands rotating in the vorticity direction during large shear deformation but also the kink bands rotate in the vorticity direction toward the parallel orientation. Therefore, it is apparent that there exists a strain amplitude above which lamellae within the kink bands become fully parallel as a result of both lamellar rotation and kink band rotation.

The significance of strain in controlling the orientation and degree of shear-induced alignment in block copolymers has been addressed previously. In particular, in the regime between the parallel and perpendicular alignment conditions, strain amplitude can be used to flip the lamellar alignment from the perpendicular to the parallel orientation.[12] Our observations of lamellar and kink band rotation under large shear strain provide direct evidence of the impact of strain on the development and relative stabilities of the parallel and transverse orientations. We hypothesize that there are three strain regimes that correspond to (1) direct transformations into the parallel orientation, (2) shear-stabilized parallel−transverse biaxial textures, and (3) transformations to the parallel orientation via a transient transverse orientation. The first regime is the lowest strain regime, in which the strain amplitude is insufficient to induce kink bands and lamellae reorient locally. Therefore, aligning lamellar block copolymers with oscillatory shear in this strain regime produces a predominately parallel orientation with a wide orientation distribution; however, this strain amplitude is insufficient to create perfectly parallel orientation. The second regime is an intermediate strain regime, in which the nearly parallel and nearly transverse orientations coexist as forward kink bands in the case of steady shear and as conjugated kink bands in the case of oscillatory shear. The third regime is the largest strain regime in which kink bands and the corresponding transverse texture transform into the parallel orientation. The specific strain amplitudes which delineate these three regimes will, of course, depend on the processing conditions (temperature and frequency), as well as the molecular parameters (molecular weight, monomeric friction coefficient, etc.) and starting morphology (defect type and density) of the block copolymer.

These three strain regimes serve to unify the observations from a number of studies and unequivocally show the importance of strain amplitude during the align-

ment process in block copolymers. Previous studies in our group on SEP(40−70) have identified the critical strain between regime 1 and 2 to be 30% at 180 °C and 0.005, 0.05, or 0.1 s^{-1}. Below this strain amplitude an isotropic sample was transformed into a predominately parallel sample of modest alignment quality. Somewhat above this strain amplitude a microphase-separated, isotropic sample was transformed into a parallel−transverse sample having a dense array of conjugated kink bands. In this paper, we have nearly accessed regime 3, where the transverse lamellae in the kink bands approach the parallel orientation, as discussed above. Work in Kornfield's group on a low molecular weight poly(styrene-*b*-isoprene) diblock copolymer has clearly identified regimes 2 and 3, by correlating in situ birefringence measurements to the presence of the parallel and transverse orientations.[13,14] Wiesners' group used a parallel plate rheometer that naturally provides a range of strain amplitudes in a single sample.[8] Their ex situ small-angle X-ray scattering data indicate a transition from a parallel−transverse biaxial texture to a predominately parallel orientation upon increasing strain, as we have described moving from regime 2 to regime 3. (In related work, Wiesner's group has recently demonstrated the importance of strain amplitude in the transformations between the parallel and perpendicular orientations near the order−disorder transition.[15]) While these comparisons are complicated by numerous experimental details, the importance of strain amplitude is evident. Strain amplitude along with temperature, duration, and frequency determines which defect transformations are activated in a sample during large-amplitude oscillatory shearing. As this work shows, modest strain amplitudes (50−100%) are capable of creating kink band defects, while larger strain amplitudes are capable of transforming kink band defects. Defect mobility and transformation provide additional mechanisms by which block copolymer microdomains can change orientation.

Effect of Strain on Tilt Boundaries. Shear strain induces a decrease in the tilt boundary angle due to rotation of both the kink band boundary and the lamellae within the kink band. This reduction in the tilt angle is accompanied by a transition in the tilt boundary morphology. As found previously for quiescent samples, larger tilt angles correspond to chevron boundaries while smaller tilt angles correspond to omega boundaries. Gido and Thomas found that this transition in the tilt boundary type occurred over a range of boundary angles. We also have observed boundaries of both types occurring at similar tilt angles; however, this coexistence window increases as the strain amplitude increases. This result indicates that shear strain increases the stability of omega-type tilt boundaries. Therefore, while chevron boundaries are more stable for 70° tilt boundaries in quiescent SEP(40−70) at 180 °C, omega boundaries are more stable for the same amount of tilt when energy is imparted to the sample via steady shear. Quantitative analysis of this shear stabilization of omega boundaries would require a modification of Matsen's current energy balance due to the added shear energy.[2]

Matsen's calculations assume complete symmetry between the two blocks of the copolymer, and subsequently, omega-shaped caps are equally as likely to form in either microdomain.[2] In contrast, the omega boundaries in SEP(40−70) exhibit omega-shaped caps predominately in the PS microdomains, while the PEP microdomains form the protrusions. This asymmetry could be associated with the lower PS volume fraction or the lower extent of entanglements across the PS microdomains. An estimate of the number of entanglements in the interpenetration zone for the PS and PEP microdomains shows that the PS microdomains are relatively unentangled (<1 entanglement per block), whereas the PEP microdomains are significantly entangled (∼10 entanglements per block).[16,17] Fewer entanglements enhance the slip within the PS microdomains and might aid the formation of the omega-shaped caps. Conversely, the topological constraints between the opposing PEP brushes might facilitate the formation of the protrusions.

The asymmetry with respect to the interpenetration zones of SEP(40−70) is further confirmed by the selective delamination of the PS microdomains upon quenching the samples (Figure 6). As described by Joanny, a finite shear velocity imposed between two interpenetrated brushes will tilt and stretch the chains in the shearing direction, which in turn will reduce the size of the interpenetrated region.[18] As the shear strain reaches some threshold, polymer chains will no longer sustain the stress, and the two brushes in the interpenetration zone will disentangle. However, disentanglement alone is insufficient to cause delamination. We suggest that the delamination is the result of *both* disentanglement and normal forces. Lamellar contraction is known to occur during shear deformation[19] and could give rise to the necessary normal forces for delamination upon cooling.[20]

Conclusions

This study follows the evolution of kink bands and kink band boundaries under steady shear strains in the range of 1−10 strain units. An overall decrease in the tilt boundary angle is observed as the strain amplitude increases, from an average of ∼85° at 1 strain unit to ∼25° at 10 strain units, further confirming lamellar rotation within the kink bands during steady shear. Furthermore, the kink bands rotate in the vorticity direction toward the parallel orientation, suggesting that kink bands will transform into the parallel orientation at sufficiently high strains. These strain-induced transformations demonstrate the importance of strain in the alignment process of block copolymers. Upon increasing the shear strain, the kink band boundaries transform from chevron boundaries to various omega-type boundaries to broken omega boundaries. The omega boundaries observed at high strains exhibit omega-shaped caps and protrusions predominately in the PS and PEP microdomains, respectively. We suspect that this is related to the lower extent of entanglement in the PS microdomain. This idea was further strengthened by the observed delamination of the PS microdomains at the highest strain amplitude.

Acknowledgment. We are grateful to Dr. D. L. Polis, currently of GE Lighting, for commenting on this manuscript. Funding was provided by NSF-DMR-YIA (9457997) and Procter and Gamble, Co.

References and Notes

(1) Gido, S. P.; Thomas, E. L. *Macromolecules* **1994**, *27*, 6137.
(2) Matsen, M. W. *J. Chem. Phys.* **1997**, *107*, 8110.
(3) Netz, R. R. A.; D.; Shick, M. *Phys. Rev. Lett.* **1997**, *79*, 1058.

(4) Polis, D. L.; Winey, K. I. *Macromolecules* **1996**, *29*, 8180.
(5) Polis, D. L.; Winey, K. I. *Macromolecules* **1998**, *31*, 3617.
(6) Kuhlmann, W. D.; Winey, K. I. *J. Appl. Phys.* **1999**, *85*, 6392.
(7) Okamoto, S.; Saijo, K.; Hashimoto, T. *Macromolecules* **1994**, *27*, 5547.
(8) Zhang, Y.; Wiesner, U. *J. Chem. Phys.* **1995**, *103*, 4784.
(9) Pinheiro, B. S.; Winey, K. I.; Hajduk, D. A.; Gruner, S. M. *Macromolecules* **1996**, *29*, 1482.
(10) Polis, D. L.; Smith, S. D.; Terrill, N. J.; Ryan, A. J.; Morse, D. C.; Winey, K. I. *Macromolecules* **1999**, *32*, 4668.
(11) Williams, D. R. M.; MacKintosh, F. C. *Macromolecules* **1994**, *27*, 7677.
(12) Gupta, V. K.; Krishnamoorti, R.; Kornfield, J. A.; Smith, S. D. *Macromolecules* **1996**, *29*, 1359.
(13) Gupta, V. K.; Krishnamoorti, R.; Chen, Z.-R.; Kornfield, J. A. *Macromolecules* **1996**, *29*, 875.
(14) Chen, Z.-R.; Kornfield, J. A.; Smith, S. D.; Grothaus, J. T.; Satkowski, M. M. *Science* **1997**, *277*, 1248.
(15) Leist, H.; Maring, D.; Thurn-Albrecht, T.; Wiesner, U. *J. Chem. Phys.* **1999**, *110*, 8225.
(16) Witten, T. A.; Leibler, L.; Pincus, P. A. *Macromolecules* **1990**, *23*, 824.
(17) Rubinstein, M.; Obukhov, S. P. *Macromolecules* **1993**, *26*, 1740.
(18) Joanny, J. F. *Langmuir* **1992**, *8*, 989.
(19) Polis, D. L.; Smith, S. D.; Ryan, A. J.; Winey, K. I. *Phys. Rev. Lett.* **1999**, *83*, 2861.
(20) Colby, R., personal communication, 1999.

MA991303K